Vision-based Thermal Comfort Quantification for HVAC Control

Wooyoung Jung[a], Farrokh Jazizadeh[b,*]

Via Department of Civil and Environmental Engineering, Virginia Tech

[a] 315B Patton Hall, 750 Drillfield Drive, Blacksburg, VA, 24061, email: jwyoungs@vt.edu
[b] 200 Patton Hall, 750 Drillfield Drive, Blacksburg, VA, 24061, email: jazizade@vt.edu
[*] Corresponding author

Abstract

This study presents a vision-based approach that employs RGB video images as the sole source for inferring thermoregulation states in the human body in response to thermal condition/sensation variations in indoor environments. The primary objective is to contribute to our envisioned thermoregulation-based HVAC control that leverages actual thermal demands from end-users' thermoregulation states for increased energy efficiency. Our approach has been proposed in the context of four constraints of feasibility and scalability: non-intrusiveness, applicability, sensitivity, and ubiquity. To this end, the approach leverages ubiquitously obtainable RGB-video images (through webcams or smartphones) and photoplethysmography (PPG), a well-known optical technique for measuring blood volume changes in the microvascular bed of skin. Specifically, the approach leverages the mechanism of controlling the blood flow to skin surface (blood vessels' dilation and constriction) to adjust heat dissipation. Given the subtle nature of PPG signals and their susceptibility to noise, we proposed a framework that uses a combination of independent component analysis and adaptive filtering to reduce unwanted and in-band artifacts while preserving the amplitude information of PPG signals. The framework was experimentally evaluated using transient thermal conditions to account for applicability and sensitivity attributes. Therefore, without considering an acclimation time for stability of thermoregulation states, human subjects were exposed to varying temperatures (~ 20 – 30°C) while reporting their thermal sensations. In total, for 10 human subjects out of 15, a positive correlation between vision-based indicators, skin temperature, and thermal sensations were observed demonstrating promising potential in inferring thermal sensations of occupants with sufficient sensitivity.

Keywords: User-centered HVAC system; Personalized thermal comfort; photoplethysmography (PPG); Thermoregulation; Adaptive filtering; Skin temperature.

1. Introduction

The major objective of heating, ventilation, and air conditioning (HVAC) systems is to provide satisfactory thermal conditions for occupants by leveraging thermal feedbacks from the environment. The feedback is commonly represented as temperature variations in an environment with implied user thermal satisfaction. Current HVAC systems are designed to use the predicted mean vote (PMV) model, promoted by standards, such as American Society of Heating, Refrigerating, and Air Conditioning Engineers (ASHRAE) standard 55 [1], as an approach for reflecting occupants' perspective. However, it has been indicated that the use of generalized metrics of the human-related parameters does reflect the characteristics of actual occupants. Consequently, a considerable portion of occupants endure thermal dissatisfaction [2] due to inaccurate thermal sensation estimation (stemmed either from PMV limitations [3-6] or inaccurate information from individuals) or over-cooling/heating [7]. Such operational limitations often bring about considerable reduction in energy efficiency of HVAC systems despite their leading contribution in driving building energy demands [8].

In addressing the aforementioned limitations, integration of post-occupancy feedback from diverse actual occupants [9] into the control loop of HVAC systems is a key step to satisfy individual thermal demands. The fast-pace growth in ubiquitous communication technologies have provided the ground for this change. This class of techniques, which is commonly called personalized (alternatively user-centered or user-led)

HVAC control, seeks to integrate thermal sensations of actual occupants into HVAC control loop through: (1) occupant voting and profiling systems (OVPS) or (2) physiological sensing technologies (PST). In the last decade, the OVPS approach has thrived by leveraging the capabilities of mobile computing technologies (such as smartphones) that provide high accessibility to contextual thermal feedback from occupants [10-12], which paved the way for personalized thermal comfort profiling [8, 13] and their applications in distributed control logic [14-16]. Although OVPS methods have contributed to personalized HVAC control, their success calls for consistent contributions from users [17, 18]. Moreover, as the survey-based methods rely on direct quantification of occupants' feedback, regardless of diverse influencing factors like thermoregulation states, the moderate accuracy (~60 – 70%) in profiling has been obtained [19, 20].

The emergence and maturity of non-intrusive and wearable sensing technologies has drawn attention to the potential of PST. In interaction with variable thermal conditions, the human body regulates a number of physiological processes (collectively known as the thermoregulation mechanisms) to maintain the constant core internal temperature. Leveraging such a mechanism, the variations in skin temperature [21-23], heart rate [24], and respiration [25-27] have been studied as potential parameters for quantifying thermophysiological responses and assessing occupants' thermal comfort. The candidate technologies for PST-based thermal comfort assessment require to be non-intrusive such as infrared imaging, Doppler radar sensors, and wearable sensors (e.g., smartwatches) to account for reduced interruptions in occupants activities [28].

In this study, following the emerging trend of PST-based methods, we have sought to investigate the feasibility of a ubiquitous and cost-effective approach for thermoregulation states inference. RGB video images are conveniently accessible via omnipresent smart computing devices. Furthermore, in their daily activities, a majority of office occupants often work in front of camera-equipped devices. If RGB video images can be used for thermal comfort assessment, they could provide a cost-effective method for PST-based thermal sensation inference. Accordingly, as the fundumental steps in this feasibility assessment, we have attempted to answer the following questions:

- Is it possible to use RGB video images, as the sole information source, to infer the thermoregulation states across a range of typical thermal sensations and their associated thermal conditions?

In our prior studies, we have examined the potential of utilizing RGB video images to assess thermoregulation states in low (20°C) versus high (30°C) thermal conditions with a prolonged acclimiaton time (20 minutes) during which the human body transitions into a steady thermoreglation state [29, 30]. The Eulerian magnification algorithm [31] that amplifies subtle skin color variations was used as the key algorithm. To further investigate the feasibility, in this study, we investigated the feasibility of using RGB video image under transient thermal conditions and therefore devised a novel framework to address the challenges associated with the subtlety of variations.

- Is video imaging analysis sufficiently sensitive to infer when a user's thermal sensation changes?

It is desirable for a building system to identify individual discomfort of the occupants and respond to it in a timely manner to adjust the indoor conditions and minimize thermal dissatisfaction. Accordingly, in the experimental studies human subjects were exposed to transient thermal condition without prolonged and unrealistic acclimation times. Given the smaller range of temperature variations that human subjects experience and the subtlety of physiological variations, we proposed to use a motion noise removal algorithm using independent component analysis (ICA) and adaptive filtering to infer the states of thermoregulation.

The rest of the paper has been structured as follows. Section 2 describes the characteristics and requirements of the envisioned thermoregulation-based HVAC operation and the association between the thermoregulation mechanism and photoplethysmography (PPG) approach, which we employed to extract indicator of thermoregulation states. The third section elaborates our proposed framework for evaluating thermoregulation states through RGB video images. The experimental procedures for investigating our objectives are described in Section 4. The fifth section presents the results, and Section 6 concludes the paper.

2. Thermoregulation-based HVAC control and motivation

This study contributes towards our vision to employ the thermoregulation mechanisms as a direct feedback to control HVAC systems. Using the correlation of physiological responses with ambient conditions, it is expected that personalized and realistic thermal demands could be quantified with minor dedication from occupants. We refer to this envisioned system as thermoregulation-based HVAC control, which infers end-users' thermoregulation states and manages indoor thermal conditions accordingly. The conceptual framework is as illustrated in Figure 1. Moving towards realization of such a system, we have investigated a potential measurement technology that uses RGB images and could be embedded in the desired system.

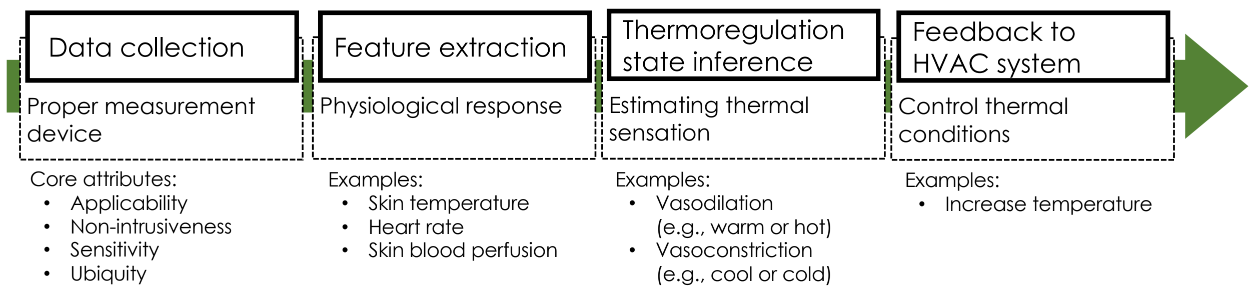

Figure 1. The envisioned framework for thermoregulation-based HVAC control

As noted, technologic developments have provided an opportunity for measuring real-time physiological responses from the human body. This is the foundation of our vision to move towards thermoregulation-based control, in which HVAC systems take occupants' thermoregulation states into account rather than measuring average temperature within a space. Moreover, the approach could account for personalized thermal sensation with reduced commitment from occupants. Realization of such feedback system calls for measurement techniques with the following attributes:

- **Applicability**: Being capable of inferring the correlation of at least one physiological parameter with the ambient thermal conditions so that thermoregulation states could be identified,
- **Non-intrusiveness**: Minimize interruptions/interference with occupants' activities,
- **Sensitivity**: Recognize subtle variations in physiological responses corresponding to thermal sensations in a timely manner so that the system can promptly respond to a discomfort state,
- **Ubiquity**: Be pervasively available to facilitate scalable data collection process and enable distributed assessment of thermal sensations in an environment.

The merits of ubiquity and non-intrusiveness that RGB video cameras offer motivated our exploration on their applicability and sensitivity, which are closely related to real-world implementation.

2.1. Photoplethysmography (PPG) technology and thermoregulation

Photoplethysmography (PPG) is our main approach in inferring thermoregulation states. PPG is commonly utilized in medical domains for non-intrusive measurement of physiological indicators (i.e., vital signs). Smart computing devices such as smartwatches have adopted PPG to provide physiological information to their users [32]. PPG methodologies rely on a light source to illuminate the tissue and a photodetector (e.g., a camera) to capture signals. In conventional PPG methods, dedicated red and/or infrared (IR) wavelengths have been used as the light source treating ambient light as an interference [33]. To tackle such interferences, in an example study, a nontransparent cover was used to minimize the influence of ambient light on PPG signals [34]. However, Verkruysse et al. [35] changed the trend by employing normal ambient light as a PPG light source. In their research effort, using a low-cost webcam, human subjects' videos were taken at a distance of 1.5 meters, and heart rate and respiration rate were identified. This study implemented the fast

Fourier transform (FFT) algorithm on the spatially averaged RGB channel values, and extracted the frequency having the maximum amplitude within the typical cardiopulmonary frequency (cardiac cycle: 0.75 – 4 Hz, pulmonary cycle: 0.1 – 0.5 Hz).

It has been also reported that the green channel has the most robust PPG information among RGB channels, since the hemoglobin absorption bands belong to yellow and green light. Leveraging this property, Poh et al. [36] further demonstrated the feasibility of using ambient light as the PPG light source for detection of heart rates. In order to eliminate the effect of the motion artifacts, they used ICA, one of the techniques for blind source separation (BSS), in processing the PPG signals before extracting heart rates. Eliminating artifacts, mostly induced by voluntary and involuntary motion, is an important preprocessing step in using the PPG methodologies [36]. Through that study, they reported that heart rates could be more accurately identified by the estimated PPG signals. Qi et al. [37] also demonstrated the feasibility of using another BSS technique, Joint BSS, to improve the accuracy of heart rate detection, using RGB pixel values, captured at a distance.

PPG signals have been also investigated in measurement of the thermophysiological responses of the human body. In his thorough review on the clinical application of PPG, Allen [38] stated that PPG waveforms contain thermoregulation information as one of the components. It has been also demonstrated that the vasoconstriction (constricting blood vessels for reduced heat dissipation) process causes a decrease in amplitude of PPG signals [39, 40]. Allen et al. [41] employed PPG to infer vasoconstriction induced by a deep inspiration gasp by extracting the signal segment, in which the amplitude of PPG decreased. Along the same line, Larsen et al. [42] explored the changes in spectral power contained in the thermoregulatory frequency band (0.01 – 0.08Hz) to examine anesthesia. These studies, with medical applications as their main objective, have used wearable sensors with dedicated light sources. However, in consideration of what has been envisioned for the HVAC system, non-intrusive physiological parameter measurements are preferable.

It has been stated that the peripheral temperature can be inferred by changes in the amplitude of PPG signals [43]. Figure 2 illustrates the underlying mechanism that enables this inference: as the ambient temperature changes, the hypothalamus sends nerve impulses to regulate the shunt vessels and arterioles. In low temperatures, the shunt vessels are expanded while arterioles are constricted (Figure 2 (a)) limiting heat dissipation from the skin surface. In high temperatures, the process is reversed (Figure 2 (b)). The adjustments in arterioles, close to the skin surface, are the key mechanism that affect the PPG signal amplitude variations: the expansion of blood vessels (i.e., increased blood volume) boosts the variation of the amplitude in PPG signal, and vice versa.

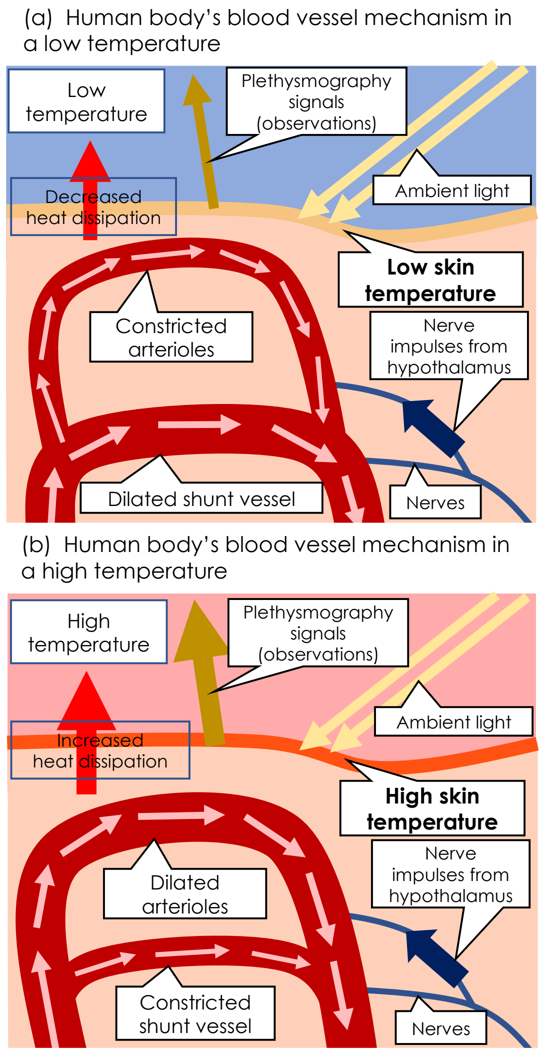

Figure 2. Thermoregulation mechanism though skin and expected PPG signal variations

Therefore, our approach utilizes non-intrusively observed PPG signals (images that are captured from a distance through a camera) to infer indicators of thermoregulation states by quantifying the variations in the amplitude of PPG signals. Furthermore, we have investigated whether the variation of PPG signal amplitude is correlated with other physiological response indicators such as skin temperature or heart rate.

3. Video thermoregulation state assessment

Our approach uses plethysmography signals, extracted from the facial skin that is sensed by red, green, and blue (RGB) sensors. This approach was inspired by the study of Poh et al. [36], in which the PPG method that uses ambient light as the PPG light source has been used for heart rate monitoring. Leveraging the adjustments of skin blood perfusion as the main thermoregulation mechanism of interest, this approach relies on the variations in plethysmography signals' amplitude that represent blood volume change in the skin tissue. Due to subtlety of the PPG signal variations and potential reduction in signal to noise ratio (SNR), we have proposed a framework that recovers the artifact-free PPG signal without compromising the amplitude information. Figure 3**Error! Reference source not found.** represents the proposed framework The following subsections elaborate on the details of each step used in Figure 3. It is important to note that this framework is a feature extraction framework and the extracted indicators of thermoregulation states cannot be deemed as absolute values in the context of this study.

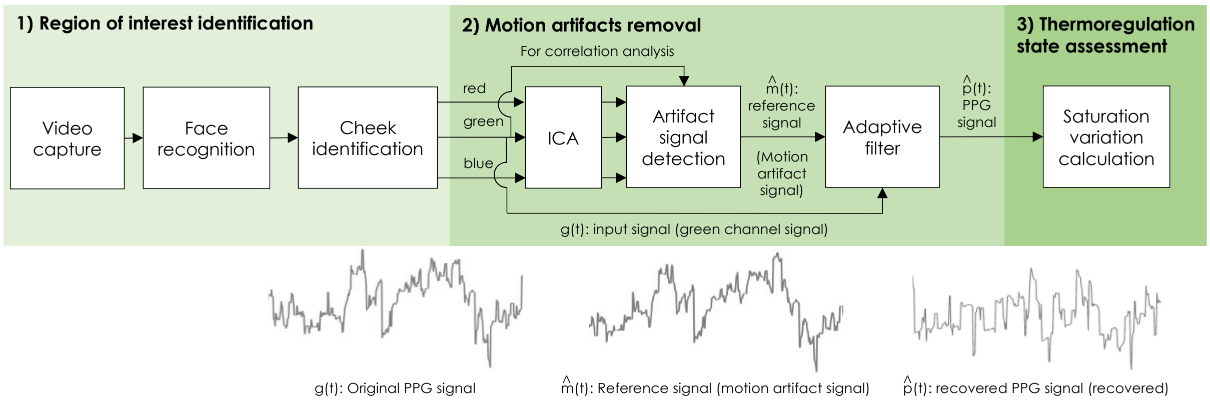

Figure 3. Block diagram of the proposed framework: Thermoregulation state assessment based on RGB video images of the face

3.1. Region of interest (ROI) identification

Given its exposure during daily activities in an indoor environment, facial skin has been selected as our region of interest. Specifically, for the purpose of this study, we have focused on the cheek area as it has been demonstrated to have a high signal-to-noise ratio (SNR) [44] and potential for higher information gain in thermal sensation analysis [21]. Moreover, the symmetry of the face, helps us measure the skin temperature for a comparative analysis. Figure 4 illustrates the configuration of the skin temperature sensor as well as an example of the area of skin pixels that were used in our PPG analysis. For the cheek pixels isolation process, we employed the Viola-Jones algorithm, a boosted cascade classifier that rapidly detects an object in images with high accuracy [45], which has been often applied to recognize face within an image [36, 46, 47]. This algorithm eliminates the unwanted background. In the second step, in this study, we have used a heuristic to extract right cheek area. Once the face is recognized in each frame, the selected frame is divided into 50 small frames (i.e. five rows and ten columns). Then, the 38th region (4th row and 8th column) is isolated as the region of interest (Figure 4). The spatial average of the RGB pixel values in each frame is used to trace raw RGB signals. Although spatial averaging brings about reduced resolution, it significantly improves the SNR [35].

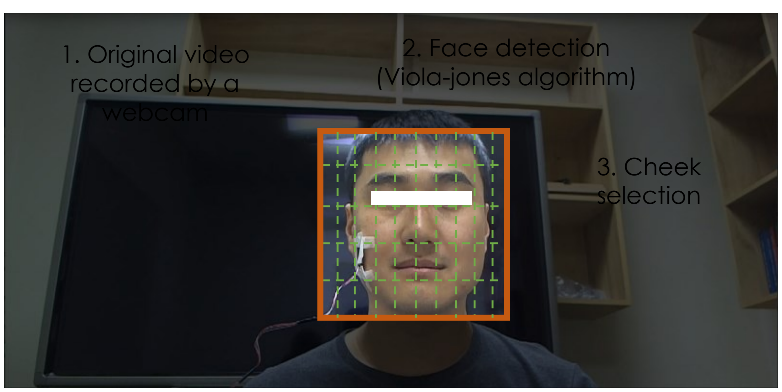

Figure 4. Region of interest (the right cheek) isolation process.

3.2. Motion artifacts removal

A key component of the proposed framework is to reduce artifacts that affect the PPG signal amplitude variations. Motion artifacts could be considered the most important source of noise in this application as it has been reported by other studies in the PPG domain [48-50]. In medical applications of PPG, accelerometer sensors are often used in combination with PPG sensing system to quantify the impact of motion. Nonetheless, our motion artifact reduction has been inspired by the study of Ram et al. [51], who proposed a novel approach for curtailing motion artifacts without an additional hardware to capture the motion signals.

As the first step in the framework, the motion noise signal is separated using ICA, which generates independent underlying source signals from the original signal – i.e., PPG and motion-artifact signals [50, 51] under the assumption that the RGB signals (i.e. the original observations) are the result of a mixture of statistically independent PPG and motion artifacts. This can be represented by

$$x(t) = As(t) \tag{1}$$

where $x(t)$ is the original color signal time series ($x(t) = [r(t), g(t), b(t)]^T$) and $s(t)$ is the source signals ($s(t) = [s_1(t), s_2(t), s_3(t)]^T$). In general, ICA generates the same number of output signals from the original set of signals [52], therefore, A is a square matrix with mixture coefficients. The objective of using ICA is to transform a set of RGB signals into the approximated source signal (i.e., $\hat{s}(t)$) as follows.

$$\hat{s}(t) = Wx(t) \tag{2}$$

where W is a demixing matrix that maximizes non-gaussianity (a key principle of ICA) for each signal [53]. We used the FastICA algorithm, one of the most widely used ICA methods [54], which achieves a very fast convergence, compared to ordinary ICA methods that utilize the gradient method [53]. In order to meausre nongaussianity, negentropy (a normalized differential entropy) was employed because it provides robust approximation. The following equations represent how the negentropy is calculated.

$$J(t) \propto [E\{G(t)\} - E\{G(v)\}]^2 \tag{3}$$

$$G(t) = -\exp(-t^2/2) \tag{4}$$

where J is negentropy, E is expectation (average), v is a gaussian variable of zero mean and unit variance (i.e., standardized).

PPG signal can be recovered by ICA [36], but the ICA-processed signal has the following limitations [55]: (1) The recovered source signals are normalized, hence they do not contain signal amplitude information, which is critical in our application, and (2) the recovered source signals have permutation ambiguity. In other words, ICA is beneficial when the objective is the frequency retrieval (e.g., retrieving heart rate), but it does not preserve the amplitude of the signal for feature extraction. Therefore, the ICA-processed PPG signal will not be sufficient for our approach. However, as indicated by Peng et al. and Ram et al. [50, 51], motion artifact signal can be estimated by ICA without the use of additional hardware. PPG signals in the raw RGB signals only represent 0.1% of total amplitude [51], so the overall shape of the raw RGB signals is mainly shaped by the artifact signals. Hence, we calculate correlation coefficients of each ICA output signal with the green channel signal to identify the artifact signal (hereinafter $\widehat{m}(t)$). As noted, green channel $g(t)$ has been demonstrated to have the most robust PPG information [35] among all channels. This process helps identify the artifact signal automatically as the order of the estimated source signals (the output of ICA) is not known and interchangeable (permutation ambiguity).

In order to recover the artifact-free PPG signal, in the next step Adaptive Filtering is utilized. Adaptive Filtering is known as one of the best options for in-band noise cancellation while maintaining the amplitude information of PPG signals [49]. Adaptive filtering requires input and reference signals to reshape the reference signal for a better match with the input signal. By using the ICA-processed motion artifact signal as the reference signal and the average green channel waveform as the input signal, the motion artifact component in the green channel signal $y(t)$ could be retrieved:

$$y(t) = w^T \widehat{m}(t) \tag{5}$$

where w is the coefficient vector, which is iteratively updated using an error signal, $\hat{p}(t)$, computed by comparing $y(t)$ the output signal with $g(t)$ input signal ($\hat{p}(t) = g(t) - y(t)$), rendering a closer match between the output signal and the input signal. In this study, we used the most widely used least mean squares (LMS) adaptive filter [56], which takes an instantaneous estimate of the mean square error as the cost function (Equation (4)).

$$w(t) = w(t-1) + \mu\hat{p}(t)\hat{m}(t) \quad (6)$$

where μ is the convergence factor that determines the step size between coefficient vectors. In the end, the PPG signal $\hat{p}(t)$ is recovered as an error signal. This procedure is illustrated in a block diagram in Figure 5.

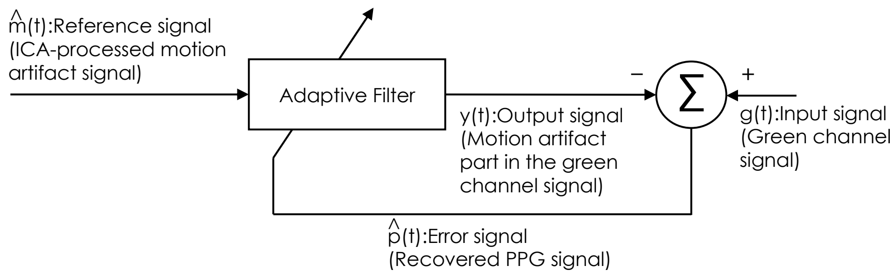

Figure 5. Block diagram of an adaptive filter and the application of this study [48].

3.3. ***Thermoregulation state evaluation*:**

In the last step of the proposed framework, the variance of the recovered PPG signal is calculated as an index representing the thermoregulation state (i.e., inferring the blood vessels conditions). We call this index pulsatile intensity (PI) (see Equation (4)).

$$PI = \frac{1}{t-1}\sum_{i=0}^{t}(\hat{p}(i) - \mu)^2 \quad (7)$$

where μ represents the mean of the PPG signal. The fluctuation of the PPG signal, presented by the variance, indicates the blood vessels' conditions that are regulated by the thermoregulation mechanism and is used as the representation for pulsatile intensity.

4. Experimental Study

An experimental study was conducted to assess the performance of the framework and address the research questions. The main objective of the experimental study was to evaluate the applicability of the proposed methodology. As its primary objective implies, the approach is expected to act as feedback for adjusting the indoor conditions based on end-users' thermal preferences. Therefore, it is desirable for the system to infer varied thermoregulation states corresponding to changes in thermal sensations. Hence, the sensitivity of the system in detection of changes is a critical factor. Several studies that have used PST-based techniques stated that physiological responses and thermal sensations of subjects become stable at least after 20 minutes [57-59]. Consequently, in these studies, an acclimation time has been often taken into account while measuring physiological processes under different thermal conditions (see Table 1 for detailed information on these studies).

The need for a prolonged acclimation time can lead to a discomfort period when it comes to real-time operation of building systems. In other words, if prolonged acclimation time is required, occupants need to endure uncomfortable thermal conditions until a building system infers the discomfort and shifts to a new control state. Therefore, in our experiments we did not consider a predefined or prolonged acclimation time prior to measurement of the physiological response of human subjects. In doing so, a transient temperature variation was employed in our experiments (from 20 to 30ºC [58]). There are precedents in adopting such an approach (i.e., using no acclimation time) in studies on association between skin temperature and thermal sensations. For example, in a study by Nagano et al. [57], they immediately exposed the human subjects to lower temperatures (22, 25, 28, and 31°C) after had been experiencing a high temperature (34 or 37°C) for 50 minutes. Once subjects experienced the lower temperature conditions, the subjects' mean skin temperatures and thermal sensations showed an immediate change. Choi and Loftness [60] also used a transient condition in identification of the body parts that provide the most robust skin temperature information for thermal comfort assessment.

Table 1. Spectrum of studies on physiological response measurements.

Measured physiological response	Measurement technique	Temperature range	Acclimation time	Reference
Skin temperature, ECG, EEG	Thermocouples, ECG, electrodes	21 – 29°C	60 Minutes	[61]
Skin temperature, ECG	Thermocouples, ECG	21 – 29°C	40 minutes	[62]
Skin temperature	Thermometer	21 – 33°C	15-20 minutes	[4]
Heart rate	Webcams	20 – 29°C	20 minutes	[24]
Heart rate variability	ECG	21 – 29°C	40 minutes	[58]
Skin temperature, heart rate, blood pressure	Thermocouples	19 – 22°C	30 minutes	[63]
Heart rate	PPG	20 – 29°C	20 minutes	[24]
Respiration	Doppler Radar	20 – 29°C	20 minutes	[25]

4.1. Experimental Set-up

We set up a thermal chamber with the dimensions of 4.2 (length) × 3.0 (width) × 2.8 (height) m^3 as our testbed. The testbed was equipped with an air handling unit, enabling us to adjust the thermal condition from low (18 – 19°C) to high (29 – 30°C) temperatures. This testbed does not have any windows, and its door opens to a corridor. Thus, the artificial lighting system was the only source for illumination. In order to quantify the ambient conditions in the room, air temperature was recorded by a DHT22 temperature/humidity sensor (± 0.5°C and ± 2 – 5% accuracy) connected to an Arduino microprocessor in the vicinity of subjects during the entire experiment. The experimental setup was designed to mirror a realistic scenario as well. In doing so, subjects were sitting <1.0 meters away from the webcam. It was a reasonable distance considering that smart devices are usually located less than 1.0 meter from users and personalized computer webcams are usually located within 1.0 meters from users' face (Figure 6). For the RGB sensor, Logitech HD Pro Webcam 920 with 30 frames per second (FPS) was used in the experiments, which represents a commonly accessible webcam technology and was proven to be comparable to cameras with higher FPS [64]. The pixel resolution for this sensor is 1080p (1,920×1,080 pixels). We also utilized a E-type thermocouple sensor that is composed of chromel and constantan, to measure facial skin temperature and a NeuLog fingertip heart rate and pulse sensor to measure subjects' heart rate.

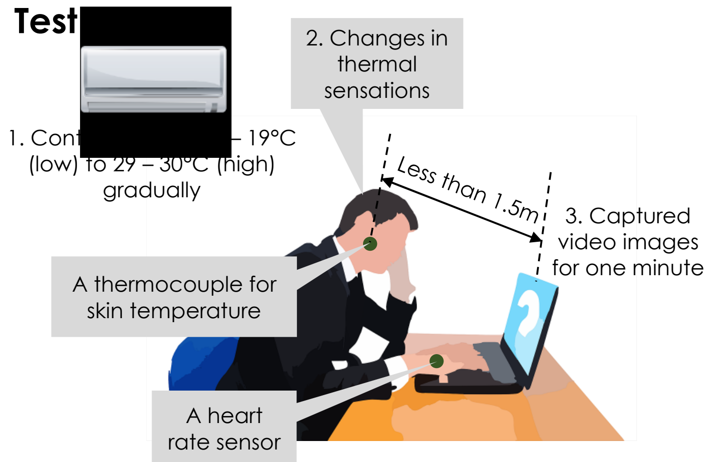

Figure 6. Testbed setup and the procedure of the experiment.

In total, 15 human subjects (eight males and seven females) were recruited in this study. All human subjects who participated in this experiment had light skin complexions. Two of the male subjects had several pimples on their face and most of female participants appeared to wear slight makeup. Although makeup could block pulsatile physiological signals, we did not provide recommendations for avoiding it in order to check the applicability of the framework regardless of the makeup. Table 2 presents the characteristics of the participants. At the time of the experiments, they declared that they were healthy with no history of cardiovascular problems that might affect the observations in the experiment. In order to ensure that the experimental procedure only reflects thermoregulation reaction in the body, participants were asked to avoid drinking alcohol a day before the experiments and any caffeine-contained drinks at least two hours prior to the experiments. They were also requested to refrain from heavy physical activities, smoking, and eating heavy meals prior to the experiments. The level of 0.5 clo (e.g. short-sleeved shirts and trousers [65]) was recommended to participants. However, we did not strictly control the combination of clothes. Most of male subjects followed the recommended clothes as intended, but some female subjects wore a skirt with long sleeve shirts. The experimental studies were conducted upon receiving the approval of Virginia Tech' Internal Review Board (IRB) and informed consent was obtained.

Table 2. Information of human subjects, participated in this experiment.

# of subject	Gender	Facial feature	# of subject	Gender	Facial feature
1	Male	None	8	Female	None
2	Male	None	9	Male	Glasses
3	Male	None	10	Female	Makeup
4	Female	None	11	Female	Makeup
5	Male	None	12	Male	None & Pimples
6	Male	None	13	Female	Makeup
7	Male	Glasses & Pimples	14	Female	Makeup & Glasses
			15	Female	Makeup

The experimental procedure included recording videos, measuring skin temperature and heart rates, and asking subjects' thermal sensations and preferences. For thermal preferences, we used an ASHARE-like thermal sensation scales with five degrees (Hot, Warm, Neutral, Cool, and Cold) as the middle degrees (–1, 0, and 1) in the ASHRAE scale represents the satisfactory condition [1]. This modified ASHRAE scale has been commonly used in other studies for personalized thermal comfort modeling [7, 12, 13]. Transient thermal conditions were simulated by gradually increasing the temperature in the testbed. We started from the low temperature. Once the low temperature was set, the human subject was asked to enter the testbed.

To eliminate the residual heat, caused by the participants' activity (mainly due to walking to the testbed), five minutes of an acclimation time was used prior to the beginning of the experiment. During this transition time, ground truth instrumentations were configured: the thermocouple sensor on the left cheek as well as the heart rate sensor on a fingertip. Two physiological responses of skin temperature and heart rate were measured during the entire experiment. At this stage, each human subject was asked to input his/her thermal sensation and a video of the facial area was captured for one minute. It is worth mentioning that we requested subjects to be as still as possible while recording their videos to reduce excessive motion artifacts. Upon collecting the initial set of data, we increased the air temperature by 1°C increment per five-minute intervals on average and human subjects were asked to declare when their thermal sensation changes. Whenever human subjects shifted their perception under the five thermal sensation criteria (cold, cool, neutral, warm, and hot), subjects were asked to report their thermal sensations through an online survey, stay stationary, and look at the webcam for one minute while we recorded their facial videos. The experiment was terminated once each human subject perceived the environment as hot and the last video data was captured.

5. Data Analytics' Results and Discussion

The framework implementation and the analyses were conducted in the MATLAB environment. Upon detection of ROI, the artifact-free PPG signal for the green channel of each video was obtained using the proposed framework. The same initial matrix for FastICA, recommended by Hyvärinen and Oja [53], and the filter length and step size parameter for the LMS adaptive filter were set through empirical observations. We employed the heuristically-identified matrix of [0.5286, 0.8449, 0.0820; 0.7338, 0.1204, 0.6686; 0.7625, 0.1625, 0.6262] and values of 512 and 0.001, respectively, which presented stable outcomes in our dataset. Thermoregulation states, represented by pulsatile intensity indicators, of each participant were calculated, and compared against air temperature, skin temperature, and heart rate at the times, when each subject changed his/her thermal sensations. The results are presented in two following subsections: (i) the relationships between temperature variation, thermal sensations, and conventional physiological responses such as skin temperature and heart rate and (ii) pulsatile intensities for different ranges of thermal sensations and their associated ambient temperatures.

5.1. Conventional Physiological Responses

Figure 7 to Figure 9 show the association between human subjects' thermal sensations with air temperature, facial skin temperature, and heart rate, respectively. As noted, facial skin temperature was measured using a heat-flux sensor array, which was attached on one of the cheeks for each human subject. As noted, due to the symmetry of the face, the cheek area was selected to provide a comparative ground for assessment of the proposed vision-based system. The sensor was not exposed to the ambient air so to ensure that the temperature values are mainly derived from skin heat flux.

When air temperature is taken into account (Figure 7), it could be observed that each participant had different thermal ranges for their thermal sensations. In other words, they manifested different thermal preferences, which is the core concept in support of the need for personalized thermal comfort quantification. Subjects revealed different thermal sensations even at the same temperature. A notable example is perception differences, observed between subject #1 and #14. At the 22.2 °C, it was cool to the former but it was already warm (almost hot) to the latter. The boxplot also illustrates that the gap between the 1st and 3rd quartiles in the warm and hot states are 3 and 4 degrees Celsius. As this figure shows, some of the participants did not perceive the environment as cold. Only five participants started with a cold perception. It is important to note that the human subjects were not aware of the temperature values in the testbed.

Another important observation in this experiment is the gap between sensitivity of individual participants. Human sensitivity to thermal condition variations is an interesting feature that could play an important role in adaptive energy management in buildings. For instance, for human subject #3, the neutral state started at 19.5°C and persisted until 25.0°C. The gap was 4.5°C. On the other hand, it was varied within 1.2°C for subject #14, who was the most sensitive participant to thermal changes. The takeaway from these observations is twofold: (1) the timeframe between perception changes for some individuals is too short and (2) different individuals have different mechanisms for response to ambient conditions and internal thermal set points.

As literature also states, skin temperature was observed to be a more reliable physiological response than the heart rate. Figure 8 shows the skin temperature values when each subject reported a change in their thermal sensations. For all subjects, the skin temperatures revealed an increasing trend along with the air temperatures during the experiments. On the other hand, as represented in Figure 9, a consistent increasing trend in the heart rates was only observed for subject #2. For subject #3, 6, 9, 10, 12, and 13, the heart rates gradually increased within a certain range (e.g. from cool to warm for subject #10), but the heart rates for other participants fluctuated. As Figure 10 demonstrates, only by grouping the data from warm and hot conditions as well as cool and cold conditions an increasing pattern for heart rate variations is observed.

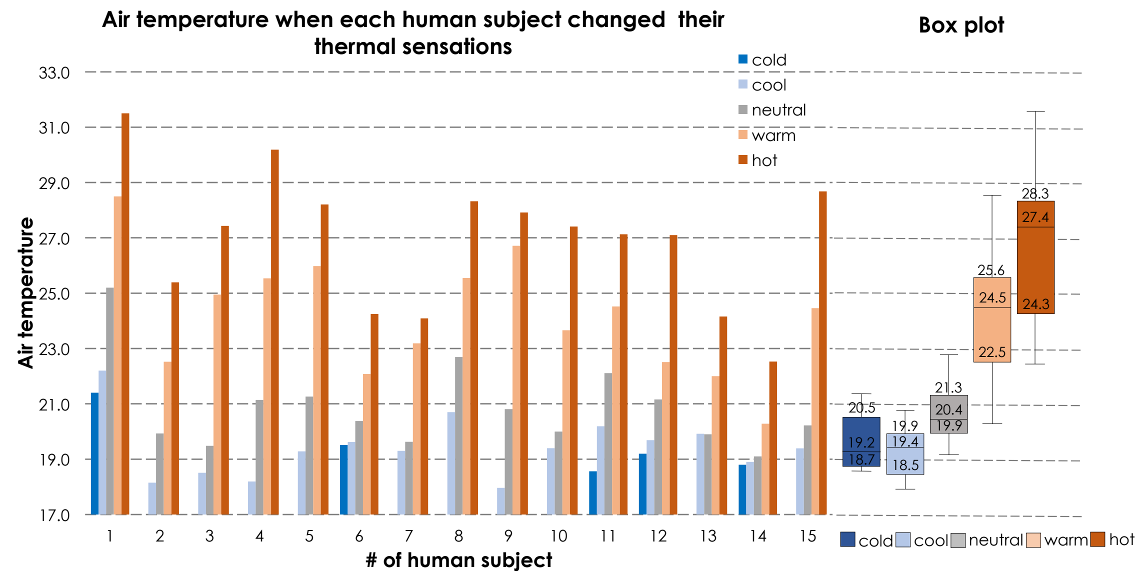

Figure 7. Air temperatures when each human subject changed their thermal sensations.

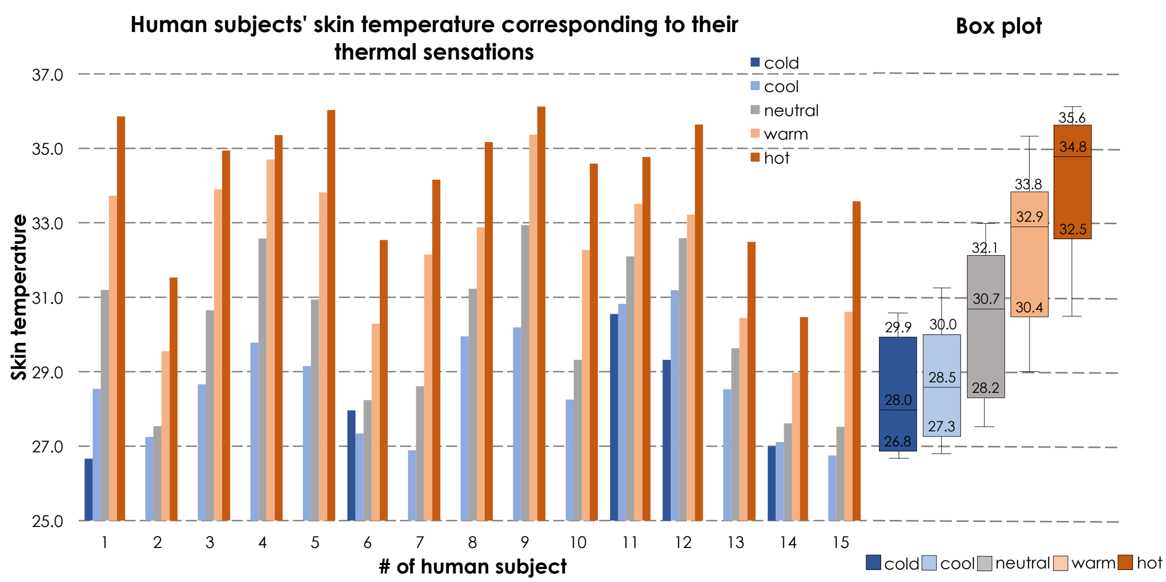

Figure 8. Cheek skin temperatures of 15 human subjects when they changed their thermal sensations.

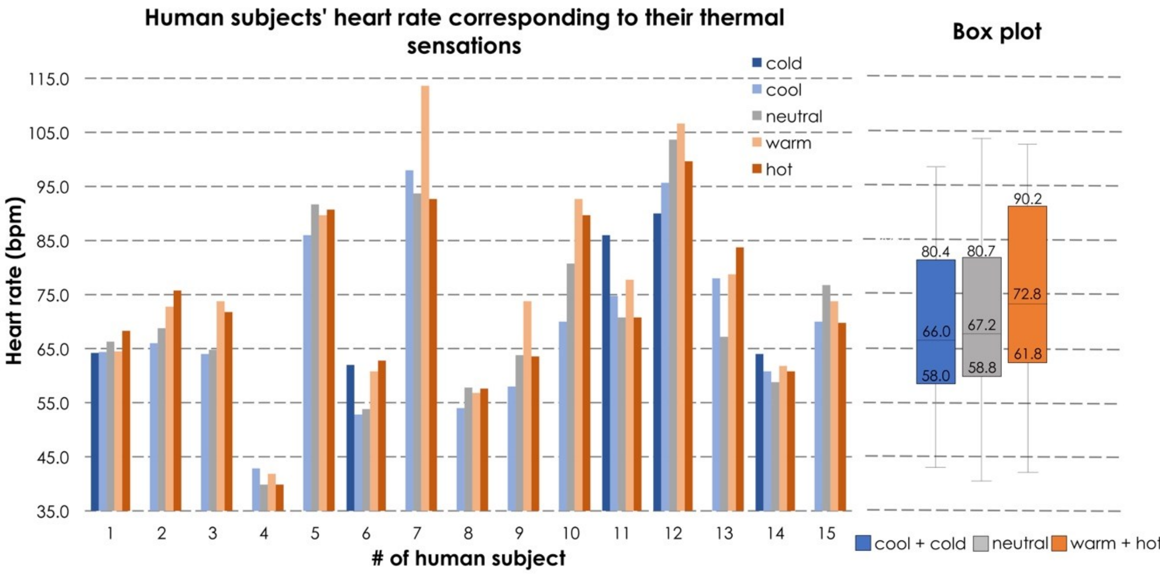

Figure 9. Heart rates of 15 human subjects extracted when they changed their thermal sensations.

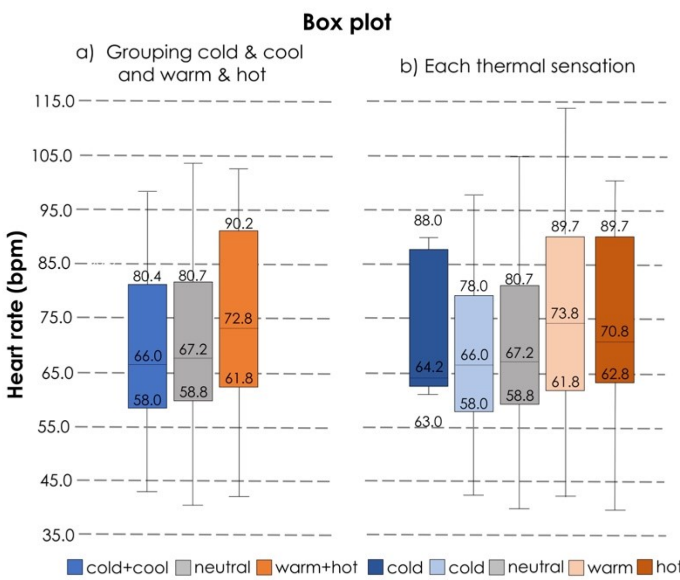

Figure 10. Box plots of the measured heart rates for 15 human subjects: (a) Grouping cold & cool and warm & hot, and (b) Each thermal sensation.

5.2. Pulsatile Intensity

As noted, the proposed framework was used to calculate the pulsatile intensity at the times that subjects expressed a change in their thermal sensations. The results of these calculations have been presented in Figure 11: (a) shows the cases with an increasing trend and (b) the cases that do not show a trend. The results showed an increasing trend for seven male and five female participants. As indicated in Figure 11 (a), for subjects #2 and 7, pulsatile intensities steadily increased from cold (cool) to hot thermal sensation states. Among these subjects were two with pimples on their face. For subject #1, 4, 5, 11, 12, 13, 15, an increasing trend was shown from cold (cool) to warm and decreased when they felt hot. Through an exploration of the PPG literature we came across Lindberg and Oberg [66] study, in which they have demonstrated that the sweat water content significantly influences the amount of PPG signal caught by a photodetector. Therefore, one possibility for our observations is that higher temperatures triggered sweating for these participants, which is another thermoregulation mechanism in high temperatures. Even though an increasing trend was observed as the ambient temperature increases at the hot state, the pulsatile intensity values were not increased at the neutral and warm states for subject #3, and slightly dropped at the warm state for subject # 9. In the case of subject 14, the pulsatile intensity increased significantly at the neutral state and remained throughout the experiment. These results demonstrated compatibility with the thermoregulation process, in which blood vessels were generally dilated to dissipate more heat as the ambient temperature increased.

Figure 11 (b) illustrates the unsuccessful cases. For subject #6, 8, and 10 the pulsatile intensities fluctuated as the temperature increased. The possible contributing factor could be the use of makeup on facial skin for subjects #10 or the distance between the subject and the camera for subject #6, who sat at the maximum limit of 1.5 meters. Consequently, the reduced quality of the images could have contributed in the observations. Nonetheless, the aforementioned circumstances could be considered as limitation of the proposed methodology.

In addition to what described above, in the interpretation of the results, a number of factors could be taken into account. As observed in the previous section, different individuals manifest different characteristics in response to thermal condition variations. As noted, the sweating process might start at higher temperatures when the subjects are feeling hot, which could affect the observations. Therefore, the visible thermoregulation processes should be also investigated in future directions of the study. Given that we have not strictly controlled the behavior (in terms of clothing insulation and the use of make-up) of the participants, 12 positive cases out of 15 shows promising results for further investigations in this direction.

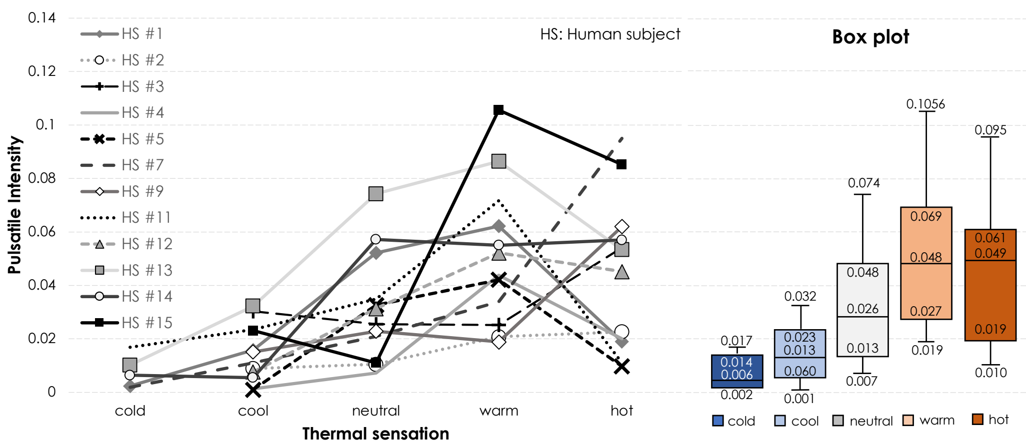

(a) Subject having an increasing tendency in pulsatile intensity.

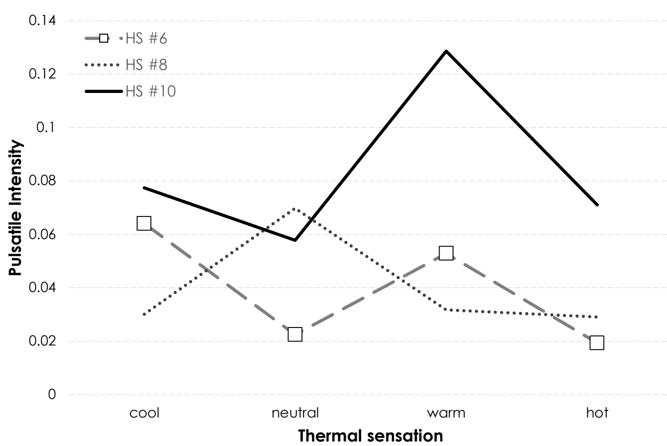

(b) Subjects having fluctuated pulsatile intensities and a decreasing tendency.

Figure 11. Pulsatile intensities of 15 subjects in different thermal sensations.

Table 3 presents the correlation coefficient of pulsatile intensity with skin temperature and heart rate. As shown in this table, the pulsatile intensities are highly correlated with skin temperature. Ten cases out of 12, for which we observed a successful performance show a strong correlation with the skin temperature variation, which is an established physiological response when it comes to thermal condition variations in an environment. In the analysis between the pulsatile intensity and skin temperature, we observed seven highly correlated cases and three moderately correlated cases. This analysis further demonstrates the promising performance of pulsatile intensity for RGB-image based thermal comfort assessment.

Table 3. Correlation coefficient analysis between pulsatile intensity, skin temperature, and heart rate.

# of subject	Correlation coefficient analysis	
	Pulsatile intensity & skin temperature	Pulsatile intensity & heart rate
1	0.5003	0.0338
2	0.9549	0.9671
3	0.5468	0.3322
4	0.7481	0.0143
5	0.2053	0.6022
6	–0.1418	–0.5147
7	0.8876	–0.2792
8	–0.3481	0.4692
9	0.6619	–0.0700
10	0.2760	0.5160
11	0.1931	0.0378
12	0.6549	0.9981
13	0.3231	–0.5832
14	0.7250	–0.5697
15	0.8146	–0.2735

Blue colored cell: highly correlated (> 0.6);
Light blue colored cell: moderately correlated (> 0.3).

6. Conclusion

We presented a vision-based approach that uses RGB videos for inferring the thermoregulation states in the human body as they correspond to the thermal condition/sensation variations in an environment. In doing so, we focused on the vasoconstriction and vasodilation mechanisms, which adjust the blood perfusion to skin vascular bed and thus the amplitude of PPG signal. This approach could contribute to our envisioned thermoregulation-based HVAC systems that evaluate actual thermal demands based on end-users' thermoregulation states. The approach was proposed in the context of four feasibility attributes: applicability, non-intrusiveness, sensitivity, and ubiquity. RGB-video images are ubiquitously obtainable through smart devices such as personal computer webcams or smartphone cameras, thereby we evaluated the remaining attributes in this study.

We proposed a framework to extract subtle amplitude variations of PPG signal by accounting for unwanted artifacts derived specifically by motion. A combination of the ICA and LMS adaptive filtering algorithms were integrated in a framework to remove the unwanted and in-band artifacts while preserving the amplitude information of the PPG signal. The variance of the PPG signal was used to assess thermoregulation states. This framework was experimentally assessed considering the interconnected attributes of applicability and sensitivity for the system integration. In the experimental study, the human subjects were exposed to transient temperature variations within the typical range of indoor temperatures

(20 – 30°C) to cover all possible thermal sensations, and an acclimation time was minimized with the aim of assessing the sensitivity. Using the proposed framework, it was demonstrated that RGB video images have the potential to be used in inferring the thermal sensations of occupants with sufficient sensitivity. In total, for 10 human subjects out of 15, a positive correlation between pulsatile intensity, skin temperature, and thermal sensations were observed. It is important to note that both physiological responses (skin temperature and pulsatile intensity) are triggered by the same thermoregulation mechanism.

However, unexpected outcomes (i.e., fluctuating trends) were also observed. There are a number of remaining challenges to be tackled for practical implementation. In another study, we asked subjects to be stationary while recording to minimize variations in light illumination and motions, which, in practice, might not be fully feasible and calls for intelligent algorithms that capture the images when subjects are focused. Moreover, distance between camera and subject plays a role. In farther distances (beyond a personal zone) the resolution of optical sensor might not be sufficient to capture amplitude variation induced by thermophysiological responses, which is also the limitation of PPG-based thermoregulation state evaluation. As demonstrated in the results, sweating and makeup could block PPG signals. Therefore, exploring the coupling of pulsatile intensities, ambient temperature, and other meta data from subjects in the context of a learning algorithm needs to be carried out in future directions of the study. On the algorithm side, although we used the most widely used ICA and adaptive filtering methods, there is still room for improving our approach. For example, the LMS adaptive filtering method calls for two user-selected inputs (i.e., filter length and step size), which can be automatically selected by the algorithm in real-time. Therefore, the future directions of this research include (1) in depth causality analysis to better understand the causes for lack of performance in some of the cases, (2) increased scale of the experiments for statistical analysis of the performance by repeating the experiments for same human subjects, (3) investigation of alternative blind source separation and adaptive filtering techniques to assess its impact on the framework's performance, and (4) system integration for HVAC control and assessment of the thermal comfort and energy efficiency implications.

7. Acknowledgement

This material is partially based upon work supported by the National Science Foundation under grant #1663513. Any opinions, findings, and conclusions or recommendations expressed in this material are those of the authors and do not necessarily reflect the views of the National Science Foundation. Authors would like to thank all the participants who participated in the experimental studies.

8. Reference

1. ASHRAE, *Thermal Environmental Conditions for Human Occupancy*. 2017, ASHRAE: Atlanta, GA.
2. Huizenga, C., S. Abbaszadeh, L. Zagreus, and E.A. Arens, *Air quality and thermal comfort in office buildings: Results of a large indoor environmental quality survey*. 2006.
3. Wong, N.H. and S.S. Khoo, *Thermal comfort in classrooms in the tropics.* Energy and buildings, 2003. **35**(4): p. 337-351.
4. Maiti, R., *Physiological and subjective thermal response from Indians.* Building and Environment, 2013. **70**: p. 306-317.
5. Becker, R. and M. Paciuk, *Thermal comfort in residential buildings – Failure to predict by Standard model.* Building and Environment, 2009. **44**(5): p. 948-960.
6. Yao, Y., Z. Lian, W. Liu, and C. Jiang, *Measurement Methods of Mean Skin Temperatures for the PMV Model.* HVAC&R Research, 2008. **14**(2): p. 161-174.
7. Sanguinetti, A., M. Pritoni, K. Slamon, and J. Morejohn. *TherMOOstat: occupant feedback to improve comfort and efficiency on a university campus*. in *American Council for an Energy-Efficient Economy Summer Study on Energy Efficiency in Buildings*. 2016. Asilomar, CA.

8. Jazizadeh, F., A. Ghahramani, B. Becerik-Gerber, T. Kichkaylo, and M. Orosz. *Personalized Thermal Comfort Driven Control in HVAC Operated Office Buildings*. in *ASCE International Workshop on Computing in Civil Engineering (IWCCE) Conference*. 2013.
9. Humphreys, M.A. and M. Hancock, *Do people like to feel 'neutral'?: Exploring the variation of the desired thermal sensation on the ASHRAE scale.* Energy and Buildings, 2007. **39**(7): p. 867-874.
10. Huizenga, C., K. Laeser, and E. Arens, *A web-based occupant satisfaction survey for benchmarking building quality*. 2002.
11. Jazizadeh, F., G. Kavulya, L. Klein, and B. Becerik-Gerber. *Continuous sensing of occupant perception of indoor ambient factors*. in *ASCE International Workshop on Computing in Civil Engineering*. 2011.
12. Jazizadeh, F., F.M. Marin, and B. Becerik-Gerber, *A thermal preference scale for personalized comfort profile identification via participatory sensing.* Building and Environment, 2013. **68**: p. 140-149.
13. Jazizadeh, F., A. Ghahramani, B. Becerik-Gerber, T. Kichkaylo, and M. Orosz, *Human-Building Interaction Framework for Personalized Thermal Comfort-Driven Systems in Office Buildings.* Journal of Computing in Civil Engineering, 2014. **28**(1): p. 2-16.
14. Jazizadeh, F., A. Ghahramani, B. Becerik-Gerber, T. Kichkaylo, and M. Orosz, *User-led decentralized thermal comfort driven HVAC operations for improved efficiency in office buildings.* Energy and Buildings, 2014. **70**: p. 398-410.
15. Daum, D., F. Haldi, and N. Morel, *A personalized measure of thermal comfort for building controls.* Building and Environment, 2011. **46**(1): p. 3-11.
16. Duan, P.-y. and H. Li. *A novel data-based control strategy of dynamic thermal comfort for inhabited environment*. in *Intelligent Control and Automation (WCICA), 2010 8th World Congress on*. 2010.
17. Jazizadeh, F. and B. Becerik-Gerber. *Toward adaptive comfort management in office buildings using participatory sensing for end user driven control*. in *Proceedings of the Fourth ACM Workshop on Embedded Sensing Systems for Energy-Efficiency in Buildings*. 2012. ACM.
18. Fukuta, M., K. Matsui, M. Ito, and H. Nishi. *Proposal for home energy management system to survey individual thermal comfort range for HVAC control with little contribution from users*. 2015. IEEE.
19. Li, D., C.C. Menassa, and V.R. Kamat, *A Personalized HVAC Control Smartphone Application Framework for Improved Human Health and Well-Being*, in *Computing in Civil Engineering 2017*. 2017.
20. Kim, J., Y. Zhou, S. Schiavon, P. Raftery, and G. Brager, *Personal comfort models: Predicting individuals' thermal preference using occupant heating and cooling behavior and machine learning.* Building and Environment, 2018. **129**: p. 96-106.
21. Ranjan, J. and J. Scott. *ThermalSense: Determining Dynamics Thermal Comfort Preferences using Thermographic Imaging*. 2016.
22. Oliveira, F.D., S. Moreau, C. Gehin, and A. Dittmar. *Infrared Imaging Analysis for Thermal Comfort Assessment*. in *2007 29th Annual International Conference of the IEEE Engineering in Medicine and Biology Society*. 2007.

23. Yi, B. and J.-H. Choi, *Facial Skin Temperature as a Proactive Variable in a Building Thermal Comfort Control System*, in *Sustainable Human–Building Ecosystems*. 2015. p. 117-125.
24. Dabiri, S. and F. Jazizadeh. *Exploring Video Based Thermal Perception Identification*. in *16th International Conference on Computing in Civil and Building Engineering, ICCCBE2016*. 2016. Osaka.
25. Jung, W. and F. Jazizadeh, *Non-Intrusive Detection of Respiration for Smart Control of HVAC System*, in *Computing in Civil Engineering 2017*. 2017: Seattle. p. 310 - 317.
26. Jung, W. and F. Jazizadeh. *Towards Integration of Doppler Radar Sensors into Personalized Thermoregulation-Based Control of HVAC*. in *4th ACM Conference on Systems for Energy-Efficient Built Environment (BuildSys' 17)*. 2017. Delft, The Netherlands: ACM.
27. Jung, W. and F. Jazizadeh, *Towards Non-intrusive Metabolic Rate Evaluation for HVAC control*, in *ICCCBE 2018*. 2018: Tampere, Finland.
28. Venkatesh, V., M.G. Morris, G.B. Davis, and F.D. Davis, *User acceptance of information technology: Toward a unified view.* MIS quarterly, 2003: p. 425-478.
29. Jazizadeh, F. and W. Jung, *Personalized Thermal Comfort through Digital Video Images for Energy-Efficient HVAC Control.* Applied Energy, 2018.
30. Jazizadeh, F. and S. Pradeep. *Can computers visually quantify human thermal comfort?* in *The third ACM International Conference on Systems for Energy-Efficient Built Environments, BuildSys 2016*. 2016. CA, USA.
31. Wu, H.-Y., M. Rubinstein, E. Shih, J. Guttag, F. Durand, and W. Freeman, *Eulerian Video Magnification for Revealing Subtle Changes in the World.* ACM Trans. Graph., 2012. **31**(4): p. 65.
32. Apple. *Your heart rate. What it means, and where on Apple Watch you'll find it.* 2017 [cited 2017 Nov 17]; Available from: https://support.apple.com/en-us/HT204666.
33. Trivedi, N.S., A.F. Ghouri, N.K. Shah, E. Lai, and S.J. Barker, *Effects of motion, ambient light, and hypoperfusion on pulse oximeter function.* Journal of Clinical Anesthesia, 1997. **9**(3): p. 179-183.
34. Hummler, H.D., A. Engelmann, F. Pohlandt, J. Högel, and A.R. Franz, *Accuracy of pulse oximetry readings in an animal model of low perfusion caused by emerging pneumonia and sepsis.* Intensive Care Medicine, 2004. **30**(4): p. 709-713.
35. Verkruysse, W., L.O. Svaasand, and J.S. Nelson, *Remote plethysmographic imaging using ambient light.* Optics Express, 2008. **16**(26): p. 21434-21445.
36. Poh, M.-Z., D.J. McDuff, and R.W. Picard, *Non-contact, automated cardiac pulse measurements using video imaging and blind source separation.* Optics Express, 2010. **18**(10): p. 10762-10774.
37. Qi, H., Z. Guo, X. Chen, Z. Shen, and Z. Jane Wang, *Video-based human heart rate measurement using joint blind source separation.* Biomedical Signal Processing and Control, 2017. **31**: p. 309-320.
38. Allen, J., *Photoplethysmography and its application in clinical physiological measurement.* Physiol Meas, 2007. **28**.
39. Kistler, A., C. Mariauzouls, and K. von Berlepsch, *Fingertip temperature as an indicator for sympathetic responses.* International Journal of Psychophysiology, 1998. **29**(1): p. 35-41.

40. Nijboer, J.A. and J.C. Dorlas, *COMPARISON OF PLETHYSMOGRAMS TAKEN FROM FINGER AND PINNA DURING ANESTHESIA.* British Journal of Anaesthesia, 1985. **57**(5): p. 531-534.
41. Allen, J., J.R. Frame, and A. Murray, *Microvascular blood flow and skin temperature changes in the fingers following a deep inspiratory gasp.* Physiological Measurement, 2002. **23**: p. 365.
42. Larsen, P.D., M. Harty, M. Thiruchelvam, and D.C. Galletly, *Spectral analysis of AC and DC components of the pulse photoplethysmograph at rest and during induction of anaesthesia.* International journal of clinical monitoring and computing, 1997. **14**(2): p. 89.
43. Peper, E., R. Harvey, I.M. Lin, H. Tylova, and D. Moss, *Is There More to Blood Volume Pulse Than Heart Rate Variability, Respiratory Sinus Arrhythmia, and Cardiorespiratory Synchrony?* Biofeedback, 2007. **35**(2): p. 54.
44. Kwon, S., J. Kim, D. Lee, and K. Park. *ROI analysis for remote photoplethysmography on facial video*. in *2015 37th Annual International Conference of the IEEE Engineering in Medicine and Biology Society (EMBC)*. 2015.
45. Viola, P. and M. Jones. *Rapid object detection using a boosted cascade of simple features*. in *Computer Vision and Pattern Recognition, 2001. CVPR 2001. Proceedings of the 2001 IEEE Computer Society Conference on*. 2001.
46. Jazizadeh, F. and S. Pradeep. *Can computers visually quantify human thermal comfort?* in *Proceedings of the 3rd ACM International Conference on Systems for Energy-Efficient Built Environments*. 2016. ACM.
47. Poh, M.Z., D.J. McDuff, and R.W. Picard, *Advancements in Noncontact, Multiparameter Physiological Measurements Using a Webcam.* IEEE Transactions on Biomedical Engineering, 2011. **58**(1): p. 7-11.
48. Ram, M.R., K.V. Madhav, E.H. Krishna, K.N. Reddy, and K.A. Reddy. *Adaptive reduction of motion artifacts from PPG signals using a synthetic noise reference signal*. in *2010 IEEE EMBS Conference on Biomedical Engineering and Sciences (IECBES)*. 2010.
49. Ram, M.R., K.V. Madhav, E.H. Krishna, K.N. Reddy, and K.A. Reddy. *On the performance of Time Varying Step-size Least Mean Squares(TVS-LMS) adaptive filter for MA reduction from PPG signals*. in *2011 International Conference on Communications and Signal Processing*. 2011.
50. Peng, F., Z. Zhang, X. Gou, H. Liu, and W. Wang, *Motion artifact removal from photoplethysmographic signals by combining temporally constrained independent component analysis and adaptive filter.* BioMedical Engineering OnLine, 2014. **13**(1): p. 50.
51. Ram, M.R., K.V. Madhav, E.H. Krishna, N.R. Komalla, and K.A. Reddy, *A Novel Approach for Motion Artifact Reduction in PPG Signals Based on AS-LMS Adaptive Filter.* IEEE Transactions on Instrumentation and Measurement, 2012. **61**(5): p. 1445-1457.
52. Hyvarinen, A., J. Karhunen, and E. Oja, *Independent component analysis* 1ed. 2001, New York: J. Wiley.
53. Hyvärinen, A. and E. Oja, *Independent component analysis: algorithms and applications.* Neural Networks, 2000. **13**(4): p. 411-430.
54. Oja, E. and Z. Yuan, *The FastICA Algorithm Revisited: Convergence Analysis.* IEEE Transactions on Neural Networks, 2006. **17**(6): p. 1370-1381.
55. Djuwari, D., D.K. Kumar, and M. Palaniswami. *Limitations of ICA for Artefact Removal*. in *2005 IEEE Engineering in Medicine and Biology 27th Annual Conference*. 2005.

56. Farhang-Boroujeny, B., *Adaptive filters: theory and applications*. Second;2. Aufl.;2;2nd; ed. 2013, Chichester, West Sussex, United Kingdom: Wiley.
57. Nagano, K., A. Takaki, M. Hirakawa, and Y. Tochihara, *Effects of ambient temperature steps on thermal comfort requirements.* International Journal of Biometeorology, 2005. **50**(1): p. 33-39.
58. Liu, W., Z. Lian, and Y. Liu, *Heart rate variability at different thermal comfort levels.* European journal of applied physiology, 2008. **103**(3): p. 361-366.
59. Chow, T.T., K.F. Fong, B. Givoni, Z. Lin, and A.L.S. Chan, *Thermal sensation of Hong Kong people with increased air speed, temperature and humidity in air-conditioned environment.* Building and Environment, 2010. **45**(10): p. 2177-2183.
60. Choi, J.-H. and V. Loftness, *Investigation of human body skin temperatures as a bio-signal to indicate overall thermal sensations.* Building and Environment, 2012. **58**: p. 258-269.
61. Yao, Y., Z. Lian, W. Liu, and Q. Shen, *Experimental study on physiological responses and thermal comfort under various ambient temperatures.* Physiology & Behavior, 2008. **93**(1–2): p. 310-321.
62. Liu, W., Z. Lian, Q. Deng, and Y. Liu, *Evaluation of calculation methods of mean skin temperature for use in thermal comfort study.* Building and Environment, 2011. **46**(2): p. 478-488.
63. Wang, Z., H. Ning, Y. Ji, J. Hou, and Y. He, *Human thermal physiological and psychological responses under different heating environments.* Journal of thermal biology, 2015. **52**: p. 177-186.
64. Sun, Y., S. Hu, V. Azorin-Peris, R. Kalawsky, and S. Greenwald, *Noncontact imaging photoplethysmography to effectively access pulse rate variability.* Journal of Biomedical Optics, 2012. **18**(6): p. 061205-061205.
65. ASHRAE, *ASHRAE Handbook Fundamentals*. 2013, Atlanta, Georgia: American Society of Heating, Refrigerating and Air-Conditioning Engineers.
66. Lindberg, L.G. and P.A. Oberg, *Photoplethysmography. Part 2. Influence of light source wavelength.* Medical & biological engineering & computing, 1991. **29**(1): p. 48-54.